Int. J. Heat Mass Transfer. Vol. 19, pp. 805–813. Pergamon Press 1976. Printed in Great Britain

FREE CONVECTION ABOUT A VERTICAL CYLINDER EMBEDDED IN A POROUS MEDIUM

W. J. MINKOWYCZ
Department of Energy Engineering, University of Illinois at Chicago Circle, Chicago, IL 60684, U.S.A.

and

PING CHENG
Department of Mechanical Engineering, University of Hawaii, Honolulu, Hawaii

(*Received* 28 *May* 1975 *and in revised form* 8 *January* 1976)

Abstract—An analysis is made for free convective flow about a vertical cylinder embedded in a saturated porous medium, where surface temperature of the cylinder varies as x^{λ}, a power function of distance from the leading edge. Within the framework of boundary-layer approximations, exact solution is obtained for the special case where surface temperature varies linearly with x, i.e. $\lambda = 1$. For other values of λ, approximate solutions based on local similarity and local non-similarity models are obtained. It is found that the local similarity solutions are sufficiently accurate for all practical purposes. Analytical expressions for local surface heat flux and overall surface heat flux are obtained.

NOMENCLATURE

A, constant defined by equation (6b);
C, constant defined by equation (58);
C_1, constant defined by equation (31c);
C_p, specific heat of the convective fluid;
D_1, constant given by equation (31d);
D_3, constant given by equation (41c);
F, transformed stream function defined by equation (17);
G, auxiliary function defined by equation (32a);
g, acceleration of gravity;
K, permeability of the porous medium;
k_m, thermal conductivity of the porous medium;
L, length of the cylinder;
P_1, quantity defined by equation (31a);
P_2, quantity defined by equation (40a);
P_3, quantity defined by equation (41a);
p, pressure;
Q, surface-integrated heat-transfer rate;
Q_1, quantity defined by equation (31b);
Q_2, quantity defined by equation (40b);
Q_3, quantity defined by equation (41b);
q, local heat transfer rate per unit area;
Ra_x, modified local Rayleigh number, $Ra_x \equiv K\rho_\infty g\beta x(T_w - T_\infty)/\mu\alpha$;
r, radial coordinate;
r_0, radius of cylinder;
S, spanwise dimension, $S = 2\pi r_0$;
T, temperature;
u, velocity component in x-direction;
u_r, reference velocity, $u_r \equiv K\rho_\infty g\beta(T_w - T_\infty)/\mu$;
v, reference velocity in r-direction;
x, axial coordinate.

Greek symbols

α, equivalent thermal diffusivity;
β, coefficient of thermal expansion;
η, pseudo-similarity variable defined by equation (15);
θ, dimensionless temperature defined by equation (18);
λ, constant defined by equation (6b);
μ, viscosity of convective fluid;
ρ, density of convective fluid;
ξ, stretched streamwise coordinate defined by equation (16);
ξ_0, constant defined by $\xi_0 \equiv (2/r_0)\sqrt{\left(\frac{\mu\alpha}{K\rho_\infty \beta g A}\right)}$;
ξ_L, constant defined by $\xi_L = (2/r_0)\sqrt{\left(\frac{\mu\alpha L}{K\rho_\infty \beta g(T_w - T_\infty)_L}\right)}$;
ϕ, auxiliary function defined by equation (32b);
ψ, stream function.

Subscripts

c, quantities associated with a cylinder;
p, quantities associated with a flat plate;
w, quantities on the surface of the cylinder;
∞, quantities at infinity.

1. INTRODUCTION

THE STUDY of free convection from the outer surface of a heated vertical cylinder embedded in a saturated porous medium has important geophysical and engineering applications. For example, as a result of volcanic activities or tectonic movements, magmatic intrusion may occur at shallow depths in the earth's crust [1]. The intrusive magma may take the form of a cylindrical shape. If the intrusive magma is trapped in an aquifer, free convective flow can be generated in the groundwater adjacent to the hot intrusives. A study of temperature distribution around the intrusives and the

associated heat flux distribution will aid in an assessment and the evaluation of geothermal resources during geophysical exploration. Furthermore, the heat-transfer coefficients obtained from this study will be useful to estimate the cooling rate of intrusive bodies and consequently the life span of a geothermal reservoir; it will also be useful to calculate the heat loss of underground casing and piping systems for the optimum design of geothermal power plants.

It has been established that a viable geothermal reservoir for power generation must have a hot heat source for the continuous supply of energy, and a highly permeable formation to ensure sustained delivery of fluids to production wells at adequate rates [2]. Under these conditions, free convective flow in geothermal reservoirs will have a high Rayleigh number. Accordingly, boundary-layer approximations, analogous to the classical viscous theory, can be applied to free convective flow in a porous medium. This has been done by Wooding [3] to treat the problem of free convection about a line source and a point source, as well as for free convection above two finite heated vertical plates embedded in a porous medium. The boundary layer approximations were also invoked by McNabb [4] to treat the problem of free convective flow in a porous medium above a horizontal heated plate. Most recently, Cheng and his co-workers [5, 6] have obtained similarity solutions for free convection in a porous medium adjacent to vertical and horizontal plates with wall temperatures being a power function of distance.

In this paper we shall study convective flow about a vertical heated cylinder embedded in a saturated porous medium, where surface temperature of the cylinder varies as x^{λ}, a power function of distance from the leading edge. Within the framework of boundary-layer approximations, exact solution is obtained for the special case where surface temperature varies linearly with x, i.e. $\lambda = 1$. For other values of λ, approximate solutions based on local similarity and local non-similarity methods [7, 8] are obtained. It is found that the local similarity solutions are sufficiently accurate for all practical purposes.

2. FORMULATION OF THE PROBLEM

Consider the problem of steady free convection about a vertical cylinder of radius r_0 and embedded in a saturated porous medium with a prescribed axial symmetric wall temperature. If we assume that (1) the convective fluid and the porous medium are everywhere in local thermodynamic equilibrium, (2) the temperature of the fluid is everywhere below boiling, (3) properties of the fluid and the porous medium are everywhere isotropic and homogeneous, and (4) Boussinesq approximation is employed, the governing equations in a cylindrical coordinate system are given by

$$\frac{\partial}{\partial r}(rv)+\frac{\partial}{\partial x}(ru)=0, \tag{1}$$

$$u=-\frac{K}{\mu}\left(\frac{\partial p}{\partial x}+\rho g\right), \tag{2}$$

$$v=-\frac{K}{\mu}\frac{\partial p}{\partial r}, \tag{3}$$

$$u\frac{\partial T}{\partial x}+v\frac{\partial T}{\partial r}=\alpha\left[\frac{1}{r}\frac{\partial}{\partial r}\left(r\frac{\partial T}{\partial r}\right)+\frac{\partial^2 T}{\partial x^2}\right], \tag{4}$$

$$\rho=\rho_\infty[1-\beta(T-T_\infty)], \tag{5}$$

where u and v are the velocity components in x and r-directions, ρ, μ and β are the density, viscosity and the thermal expansion coefficient of the fluid, K is the permeability of the saturated porous medium, $\alpha = k_m/(\rho C_p)_f$ is the equivalent thermal diffusivity where k_m denoting the thermal conductivity of the saturated porous medium and $(\rho C_p)_f$ the density and specific heat of the fluid. T, p and g are respectively the temperature, pressure and the gravitational acceleration. The subscript "∞" denotes the condition at infinity. The appropriate boundary conditions for the problem are

$$r=r_0, \quad v=0, \quad T=T_w=T_\infty+Ax^{\lambda}, \tag{6a, b}$$

$$r\to\infty, \quad u=0, \quad T=T_\infty, \tag{7a, b}$$

where $A>0$. In equation (6b) we have assumed that the prescribed wall temperature is a power function of distance from the leading edge.

The continuity equation is automatically satisfied by introducing the stream function ψ as

$$ru=\frac{\partial\psi}{\partial r} \quad \text{and} \quad rv=-\frac{\partial\psi}{\partial x}. \tag{8}$$

The governing equations and boundary conditions in terms of ψ and T are given by

$$\frac{\partial}{\partial r}\left(r\frac{\partial\psi}{\partial r}\right)+\frac{1}{r}\frac{\partial^2\psi}{\partial x^2}=\frac{\rho_\infty\beta Kg}{\mu}\frac{\partial T}{\partial r}, \tag{9}$$

$$\frac{\partial\psi}{\partial r}\frac{\partial T}{\partial x}-\frac{\partial\psi}{\partial x}\frac{\partial T}{\partial r}=\alpha\left[\frac{\partial}{\partial r}\left(r\frac{\partial T}{\partial r}\right)+r\frac{\partial^2 T}{\partial x^2}\right], \tag{10}$$

and

$$r=r_0, \quad \frac{\partial\psi}{\partial x}=0, \tag{11}$$

$$r\to\infty, \quad \frac{\partial\psi}{\partial r}=0, \tag{12}$$

with the remaining two boundary conditions for T being given by equations (6b) and (7b).

3. BOUNDARY-LAYER EQUATIONS

The boundary-layer approximations similar to those by Wooding [3], McNabb [4], Cheng and Minkowycz [5] and Cheng and Chang [6] can now be applied if we assume that convection takes place within a thin layer adjacent to the vertical surface of the cylinder. With these simplifications, equations (9) and (10) become

$$\frac{\partial}{\partial r}\left(\frac{1}{r}\frac{\partial\psi}{\partial r}\right)=\frac{\rho_\infty\beta gK}{\mu}\frac{\partial T}{\partial r}, \tag{13}$$

and

$$\alpha\frac{\partial}{\partial r}\left(r\frac{\partial T}{\partial r}\right)=\left(\frac{\partial\psi}{\partial r}\frac{\partial T}{\partial x}-\frac{\partial\psi}{\partial x}\frac{\partial T}{\partial r}\right). \tag{14}$$

We now attempt to transform equations (13) and (14) into a set of ordinary differential equations. For this purpose we introduce the following new dimensionless variables

$$\eta = \left(\frac{K\rho_\infty g\beta(T_w - T_\infty)}{\mu\alpha x}\right)^{\frac{1}{4}} \cdot \left[\frac{r_0}{2}\left(\frac{r^2}{r_0^2} - 1\right)\right] = \frac{(Ra_x)^{\frac{1}{4}}}{x}\left[\frac{r_0}{2}\left(\frac{r^2}{r_0^2} - 1\right)\right], \quad (15)$$

$$\xi = \frac{2}{r_0}\left(\frac{\mu\alpha x}{K\rho_\infty \beta g(T_w - T_\infty)}\right)^{\frac{1}{4}} = \frac{2x}{r_0}\frac{1}{(Ra_x)^{\frac{1}{4}}}, \quad (16)$$

where $Ra_x \equiv K\rho_\infty g\beta x(T_w - T_\infty)/\mu\alpha$ is the modified local Rayleigh number in a saturated porous medium. It is worth mentioning that for a thin boundary layer where r does not differ appreciably from r_0, the quantity inside the brackets in equation (15) reduces to y (where $y = r - r_0$) and consequently η reduces to the flat plate similarity variable given in [5]. Next we introduce the dimensionless stream function and temperature F and θ given by

$$\psi = r_0\left(\frac{\alpha K\rho_\infty g\beta(T_w - T_\infty)x}{\mu}\right)^{\frac{1}{4}} F(\xi,\eta) = \alpha r_0 (Ra_x)^{\frac{1}{4}} F(\xi,\eta), \quad (17)$$

$$\theta(\xi,\eta) = \frac{T - T_\infty}{T_w - T_\infty}, \quad (18)$$

which are identical to the relations for a flat plate [5] except that F is now a function of both ξ and η, and r_0 is introduced to give proper dimension for ψ.

It can be shown that velocity components in terms of the new variables are

$$u = \frac{K\rho_\infty \beta g(T_w - T_\infty)}{\mu} F_\eta, \quad (19)$$

and

$$v = \frac{r_0}{2r}\left(\frac{\alpha K\rho_\infty \beta g(T_w - T_\infty)}{\mu x}\right)^{\frac{1}{4}} \times [(1-\lambda)(\eta F_\eta - \xi F_\xi) - (1+\lambda)F], \quad (20)$$

whereas the governing equations (13) and (14) with appropriate boundary conditions in terms of the new variables are

$$F_{\eta\eta} = \theta_\eta, \quad (21)$$

$$\frac{\partial}{\partial\eta}\left[(1+\xi\eta)\frac{\partial\theta}{\partial\eta}\right] + \frac{(1+\lambda)}{2}F\theta_\eta - \lambda F_\eta\theta = \frac{1-\lambda}{2}\xi(F_\eta\theta_\xi - \theta_\eta F_\xi), \quad (22)$$

$$F(\xi,0) = 0, \quad \theta(\xi,0) = 1, \quad (23a, b)$$

$$F'(\xi,\infty) = 0, \quad \theta(\xi,\infty) = 0. \quad (24a, b)$$

It is worth noting that equations (21) and (22) are identical to those for free convection about a vertical flat plate [5] if $\xi = 0$. Thus, any deviation from $\xi = 0$ is a measure of transverse curvature effects. We shall now obtain approximate solutions for $\lambda \neq 1$ and exact solutions for $\lambda = 1$.

4. APPROXIMATE SOLUTIONS FOR $\lambda \neq 1$

(A) *Local similarity solution*

When the value of ξ or the values of θ_ξ and F_ξ are both small, the RHS of equation (22) can be deleted. With this approximation, equations (21)–(24) do not have derivatives with respect to ξ and thus can be considered as a coupled pair of ordinary differential equations with ξ regarded as a prescribed parameter. This is the so-called local similarity approximation. Thus, the local similarity equations are given by

$$F'' = \theta', \quad (25)$$

and

$$(1+\xi\eta)\theta'' + \left(\xi + \frac{1+\lambda}{2}F\right)\theta' - \lambda F'\theta = 0, \quad (26)$$

with boundary conditions given by

$$F(\xi,0) = 0, \quad \theta(\xi,0) = 1, \quad (27a, b)$$

$$F'(\xi,\infty) = 0, \quad \theta(\xi,\infty) = 0, \quad (28a, b)$$

where the primes denote partial differentiation with respect to η. We now obtain numerical solution to equations (25) and (26) by an integral method. To this end, we first integrate equation (25) and impose conditions (27a) and (27b) to give

$$F(\xi,\eta) = \int_0^\eta \theta(\xi,\eta)\,d\eta. \quad (29)$$

We now turn our attention to equation (26) which can be considered as a second-order ordinary differential equation for θ. The solution for θ is given by

$$\theta(\xi,\eta) = \int_0^\eta \left[\int_0^\eta Q_1(\xi,\eta)\exp\left\{\int_0^\eta P_1(\xi,\eta)\,d\eta\right\} + C_1\right] \times \exp\left\{-\int P_1(\xi,\eta)\,d\eta\right\} d\eta + D_1, \quad (30)$$

where

$$P_1(\xi,\eta) \equiv \left[\xi + \frac{1+\lambda}{2}F(\xi,\eta)\right] \Big/ (1+\xi\eta), \quad (31a)$$

$$Q_1(\xi,\eta) \equiv \frac{\lambda F'\theta}{1+\xi\eta} = \frac{\lambda\theta^2}{1+\xi\eta}, \quad (31b)$$

$$C_1 \equiv -\frac{D_1 + \int_0^\infty \left[\exp\left\{-\int P_1\,d\eta\right\}\int Q_1 \exp\left\{\int P_1\,d\eta\right\} d\eta\right] d\eta}{\int_0^\infty \exp\left\{-\int P_1\,d\eta\right\} d\eta}, \quad (31c)$$

and

$$D_1 = 1, \quad (31d)$$

with constants (31c) and (31d) obtained by imposing equation (30) with boundary conditions (27) and (28).

By assigning a successive value of ξ and assuming initial profile for θ, values of stream function and temperature at a particular location (ξ,η) can be obtained by iteration from the integrals given by equations (29) and (30). The solution thus obtained is an approximate one since some terms in the energy equation are assumed to be small.

(B) *Local non-similarity solution*

More accurate results can be obtained by the so-called local non-similarity solution which retains the full energy equation. To this end, we let

$$G(\xi,\eta)\equiv\frac{\partial F}{\partial\xi}, \tag{32a}$$

$$\phi(\xi,\eta)\equiv\frac{\partial\theta}{\partial\xi}, \tag{32b}$$

and equations (21) and (22) can be rewritten as

$$F''=\theta', \tag{33}$$

$$(1+\xi\eta)\theta''+\left(\xi+\frac{1+\lambda}{2}F+\frac{1-\lambda}{2}\xi G\right)\theta' = \lambda F'\theta+\frac{1-\lambda}{2}\xi F'\phi. \tag{34}$$

It is noted that equations (33) and (34) do not have derivatives with respect to ξ. However, we now have four unknowns and therefore two more equations are needed. For this purpose, we differentiate equations (33) and (34) with respect to ξ to give

$$G''=\phi', \tag{35}$$

$$(1+\xi\eta)\phi''+\left(\xi+\frac{1+\lambda}{2}F\right)\phi'=\left(\frac{1+\lambda}{2}\right)F'\phi+\lambda G'\theta -(1+G)\theta'-\eta\theta''+\frac{1-\lambda}{2}\xi\frac{\partial}{\partial\xi}(F'\phi-\theta'G), \tag{36}$$

where we have made use of equation (32).

If the last term of equation (36) vanishes, equations (33)–(36) can be considered as a set of coupled ordinary differential equations with ξ regarded as a parameter. The last term is vanishing small if either ξ or $(\partial/\partial\xi)(F'\phi-\theta'G)$ is small.

If the last term in equation (36) is deleted, we have

$$(1+\xi\eta)\phi''+\left(\xi+\frac{1+\lambda}{2}F\right)\phi'=\left(\frac{1+\lambda}{2}\right)F'\phi +\lambda G'\theta-(1+G)\theta'-\eta\theta''. \tag{37}$$

Equations (33)–(35) and (37) are referred to as the first level of truncation of a local non-similarity model, which can be considered as four coupled ordinary differential equations for F, θ, G and ϕ with ξ regarded as a parameter. These equations are to be solved subject to the following boundary conditions

$$F(\xi,0)=0,\quad \theta(\xi,0)=1, \tag{38a}$$

$$F'(\xi,\infty)=0,\quad \theta(\xi,\infty)=0, \tag{38b}$$

$$G(\xi,0)=0,\quad \phi(\xi,0)=0, \tag{38c}$$

$$G'(\xi,\infty)=0,\quad \phi(\xi,\infty)=0. \tag{38d}$$

Thus the local non-similarity solution retains the full energy equation with approximations made in a subsidiary equation, and therefore, the local non-similarity solution is expected to be more accurate than the local similarity solution.

Numerical solution to the local non-similarity equations can also be obtained by the integral method described previously for the local similarity solution. Integrating equations (33) and (35) we have

$$F(\xi,\eta)=\int_0^\eta\theta(\xi,\eta')\,d\eta', \tag{39a}$$

$$G(\xi,\eta)=\int_0^\eta\phi(\xi,\eta')\,d\eta'. \tag{39b}$$

The solution to equation (34) is identical to equation (30) in form, but with P_1 and Q_1 replaced by P_2 and Q_2 where

$$P_2(\xi,\eta)=\left(\xi+\frac{1+\lambda}{2}F+\frac{1-\lambda}{2}\xi G\right)\Big/(1+\xi\eta), \tag{40a}$$

$$Q_2(\xi,\eta)=\left(\lambda F'\theta+\frac{1-\lambda}{2}\xi F'\phi\right)\Big/(1+\xi\eta). \tag{40b}$$

Similarly, the solution to equation (37) is also given by equation (30), but with P_1, Q_1, and D_1 replaced by P_3, Q_3 and D_3 where

$$P_3(\xi,\eta)=\left(\xi+\frac{1+\lambda}{2}F\right)\Big/(1+\xi\eta), \tag{41a}$$

$$Q_3(\xi,\eta)=\left[\frac{1+\lambda}{2}F'\phi+\lambda G'\theta+(1+G)\theta' -\eta(Q_2-P_2\theta')\right]\Big/(1+\xi\eta), \tag{41b}$$

$$D_3=0. \tag{41c}$$

By assigning a value for ξ and with an initial guess of θ and ϕ, solutions to F, G, θ, and ϕ can be obtained by iteration.

Presumably, more accurate results can be obtained by introducing subsidiary equations from successive differentiation of the energy equation and deleting the terms involving ξ derivatives in the last subsidiary equation. From the previous work by Sparrow and Yu [7] and by Minkowycz and Sparrow [8], it is shown that the first level of truncation of the local non-similarity solution is sufficiently accurate, and therefore, higher levels of truncations have not been pursued in this paper.

5. EXACT SOLUTION FOR $\lambda = 1$

It is interesting to note that exact solution for equations (13) and (14) are possible if wall temperature varies linearly with height. For the special case of $\lambda = 1$, equations (15)–(18) are given by

$$\eta=\left(\frac{K\rho_\infty g\beta A}{\mu\alpha}\right)^{\frac{1}{4}}\left[\frac{r_0}{2}\left(\frac{r^2}{r_0^2}-1\right)\right], \tag{42}$$

$$\xi_0=\frac{2}{r_0}\left(\frac{\mu\alpha}{K\rho_\infty g\beta A}\right)^{\frac{1}{4}} \tag{43}$$

$$\psi=r_0\left(\frac{\alpha K\rho_\infty g\beta A}{\mu}\right)^{\frac{1}{4}}xF(\eta), \tag{44}$$

$$\theta(\eta)\equiv\frac{T-T_\infty}{Ax}, \tag{45}$$

where both η and ξ_0 are independent of x, with η depending only on r, and ξ_0 is a constant. Furthermore, for $\lambda = 1$, the RHS of equation (22) vanishes exactly.

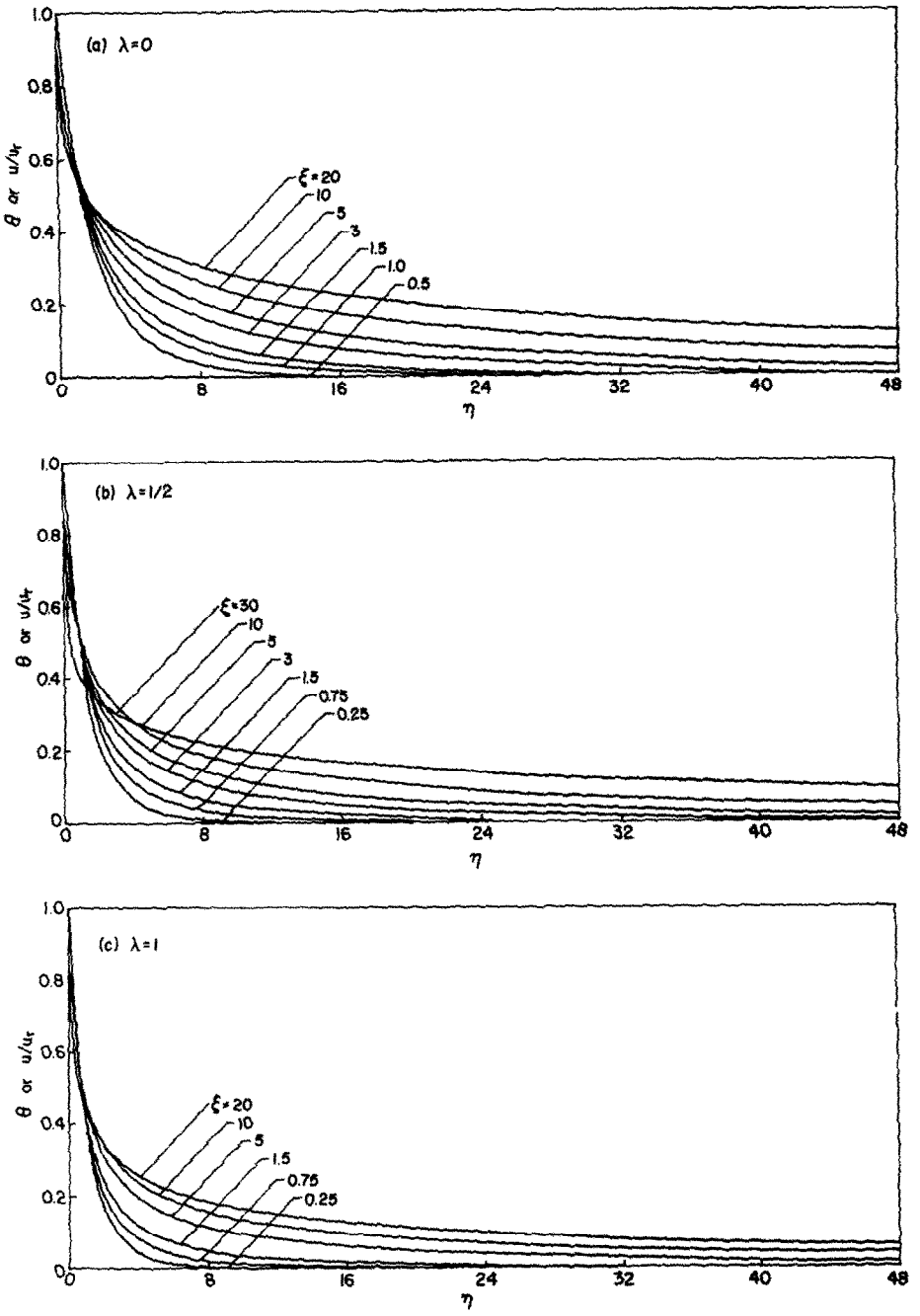

FIG. 1. Dimensionless temperature and vertical velocity profiles: (a) $\lambda = 0$, (b) $\lambda = 1/2$, and (c) $\lambda = 1$.

Thus equations (21) and (22) become

$$F_{\eta\eta} = \theta_\eta, \tag{46}$$

$$\frac{\partial}{\partial\eta}\left[(1+\xi_0\eta)\frac{\partial\theta}{\partial\eta}\right] + F\theta_\eta - F_\eta\theta = 0, \tag{47}$$

$$F(0) = 0, \quad \theta(0) = 1, \tag{48}$$

$$F'(\infty) = 0, \quad \theta(\infty) = 0. \tag{49}$$

Equations (46)–(49) are identical to equations (25)–(28) with $\lambda = 1$ and $\xi = \xi_0$. Thus the solutions to the local similarity solution is an exact one for $\lambda = 1$, and is an approximate one for $\lambda \neq 1$.

6. RESULTS AND DISCUSSION

Computations for local similarity solutions given by equations (25)–(28) as well as the first level truncation of the local non-similarity solutions given by equations (33)–(35) and equations (37)–(38) are carried out for $\lambda = 0$, 1/4, 1/3, 1/2 and 3/4. Exact numerical solution given by equations (46)–(49) for $\lambda = 1$ are also obtained for the range of ξ_0 from 0 to 20. According to equations (21) and (24), the values of θ and F' (where $F' = u/u_r$ and $u_r \equiv \rho_\infty g\beta K(T_w - T_\infty)/\mu$) are the same for any η. Thus these values are plotted as the vertical coordinate in Fig. 1. The difference in values between

Table 1. Values of $[-\theta'(\xi, 0, \lambda)]$

	$\lambda = 0$		$\lambda = 1/4$		$\lambda = 1/3$		$\lambda = 1/2$		$\lambda = 3/4$		$\lambda = 1$
ξ	LS*	LNS†	LS*	LNS†	LS*	LNS†	LS*	LNS†	LS*	LNS†	Exact
0.25	0.4855	0.4899	0.6748	0.6729	0.7234	0.7240	0.8177	0.8167	0.9383	0.9385	1.046
0.50	0.5272	0.5332	0.7186	0.7175	0.7672	0.7688	0.8620	0.8616	0.9832	0.9837	1.091
0.75	0.5664	0.5747	0.7609	0.7604	0.8096	0.8120	0.9050	0.9052	1.026	1.028	1.135
1.00	0.6049	0.6149	0.8021	0.8023	0.8510	0.8540	0.9471	0.9478	1.069	1.071	1.179
2.00	0.7517	0.7668	0.9587	0.9607	1.009	1.014	1.106	1.110	1.233	1.235	1.345
3.00	0.8915	0.9085	1.106	1.110	1.158	1.164	1.259	1.263	1.387	1.390	1.502
4.00	1.024	1.044	1.268	1.252	1.301	1.308	1.405	1.409	1.537	1.540	1.654
5.00	1.154	1.176	1.381	1.391	1.441	1.449	1.549	1.553	1.683	1.687	1.803
6.00	1.283	1.305	1.518	1.529	1.580	1.589	1.691	1.696	1.829	1.833	1.952
7.00	1.413	1.435	1.655	1.667	1.727	1.729	1.835	1.839	1.976	1.980	2.102
8.00	1.544	1.565	1.795	1.806	1.868	1.870	1.980	1.984	2.124	2.128	2.253
9.00	1.678	1.696	1.937	1.947	2.006	2.013	2.127	2.130	2.276	2.278	2.407
10.00	1.815	1.830	2.083	2.091	2.153	2.159	2.278	2.280	2.429	2.432	2.564

*LS—Local similarity solution.
†LNS—Local non-similarity solution.

the local similarity solution and the local non-similarity solution is too small to be plotted in the figures. It is shown in these figures that both the dimensionless temperature and vertical velocity have a maximum value of 1 at $\eta = 0$; their values decrease as η is increased. The boundary-layer thickness is shown to be increasing when either λ is decreased or ξ is increased. The magnitude of temperature gradient at the wall, i.e. $[-\theta'(\xi, 0, \lambda)]$, is shown to be increasing as ξ or λ is increased. The variation of $[-\theta'(\xi, 0, \lambda)]$ with respect to ξ and λ are also tabulated in Table 1.

The local surface heat flux can be computed from

$$q_c = -k_m\left(\frac{\partial T}{\partial r}\right)_{r=r_0}, \tag{50}$$

which can be expressed in terms of dimensionless variables to give

$$q_c(x) = k_m A^{3/2}\left(\frac{\rho_\infty g\beta K}{\mu\alpha}\right)^{\frac{1}{2}} \cdot x^{(3\lambda-1)/2}[-\theta'(\xi, 0, \lambda)], \tag{51}$$

where it should be noted that $\xi = \xi_0$ for $\lambda = 1$. Equation (51) is identical to the corresponding expression for free convection about a vertical flat plate [5] if the quantities $[-\theta'(\xi, 0, \lambda)]$ is replaced by $[-\theta'(0, \lambda)]$. It follows, therefore, the ratio of the surface heat flux along a vertical cylinder to that of a flat plate embedded in the same porous medium and with the same wall temperature variation is given by

$$\frac{q_c(x)}{q_p(x)} = \frac{[-\theta'(\xi, 0, \lambda)]}{[-\theta'(0, \lambda)]}, \tag{52}$$

where the subscripts "c" and "p" are used to denote the quantities associated with a cylinder and a flat plate respectively. Numerical results for equation (52) based on both local similarity solution and local non-similarity solution are tabulated in Table 2 and are also plotted in Fig. 2 where it is shown that the difference in values is maximum for $\lambda = 0$ and decrease to zero as λ approaches 1. For a fixed value of ξ, the local heat flux ratio decreases as λ increases. For a fixed value of λ, the local heat flux ratio increases quadratically for $0 \leqslant \xi \leqslant 3$ and increases linearly when $\xi > 3$.

The overall surface heat flux for a cylinder with a length L can be computed from

$$Q_c = S\int_0^L q_c(x)\,dx, \tag{53}$$

where S is the spanwise dimension which is equal to $2\pi r_0$ for a cylinder with radius r_0. Substituting equation (51) into equation (53) and performing the integration, we have

$$Q_c = \begin{cases} Sk_m A^{3/2}\left(\dfrac{\rho_\infty g\beta K}{\mu\alpha}\right)^{\frac{1}{2}} \cdot \dfrac{L^2}{2}[-\theta'(\xi_0, 0)], \text{ for } \lambda = 1, & \text{(54a)} \\ Sk_m A^{3/2}\left(\dfrac{2}{1-\lambda}\right)\left(\dfrac{\rho_\infty g\beta K}{\mu\alpha}\right)^{\frac{1}{2}} \\ \quad \times \xi_L^{-(3\lambda+1)/(1-\lambda)} L^{(3\lambda+1)/2}\int_0^{\xi_L} \xi^{4\lambda/(1-\lambda)} \\ \quad \times [-\theta'(\xi, 0, \lambda)]\,d\xi, \text{ for } \lambda \neq 1, & \text{(54b)} \end{cases}$$

where

$$\xi_L \equiv \frac{2}{r_0}\left(\frac{\mu\alpha L}{K\rho_\infty \beta g(T_w - T_\infty)_L}\right).$$

It is noted that the integration for $\lambda = 1$ can be carried out explicitly since ξ_0 is a constant and independent of x.

We now consider the ratio of total surface heat transfer for a vertical cylinder to that of a vertical flat plate with the same length embedded in a porous medium. The total surface heat flux for a vertical flat plate with a length L and a width $S = 2\pi r_0$ embedded in a porous medium is given by [5]

$$Q_p = Sk_m A^{3/2}\left(\frac{\rho_\infty g\beta K}{\mu\alpha}\right)^{\frac{1}{2}} \cdot \left(\frac{2}{1+3\lambda}\right) L^{(1+3\lambda)/2}[-\theta'(0, \lambda)]. \tag{55}$$

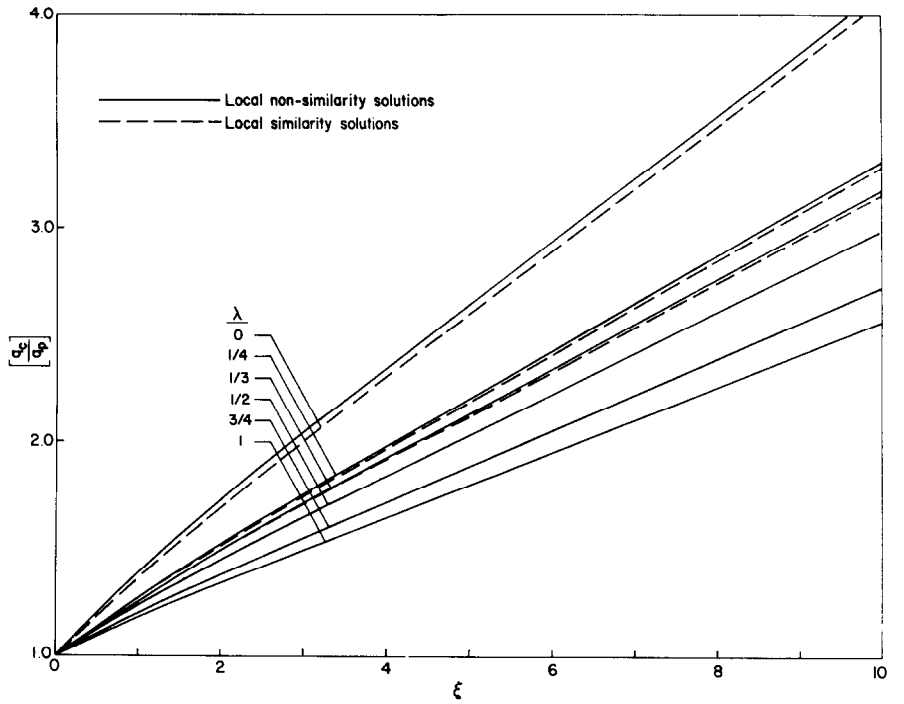

FIG. 2. Local heat-transfer ratio for selected values of λ.

Table 2. Local heat flux ratio, $q_c(\xi)/q_p(\xi)$

	$\lambda = 0$		$\lambda = 1/4$		$\lambda = 1/3$		$\lambda = 1/2$		$\lambda = 3/4$		$\lambda = 1$
ξ	LS*	LNS†	LS*	LNS†	LS*	LNS†	LS*	LNS†	LS*	LNS†	Exact
0.00	1.000	1.000	1.000	1.000	1.000	1.000	1.000	1.000	1.000	1.000	1.000
0.50	1.183	1.202	1.140	1.140	1.132	1.132	1.125	1.125	1.101	1.101	1.090
1.00	1.362	1.386	1.271	1.272	1.257	1.258	1.241	1.242	1.200	1.200	1.178
1.50	1.531	1.561	1.399	1.400	1.371	1.372	1.350	1.351	1.294	1.294	1.262
2.00	1.696	1.727	1.520	1.522	1.486	1.488	1.450	1.452	1.383	1.384	1.343
2.50	1.853	1.889	1.637	1.641	1.597	1.601	1.549	1.552	1.469	1.470	1.420
3.00	2.005	2.044	1.753	1.759	1.707	1.712	1.648	1.652	1.554	1.556	1.496
4.00	2.304	2.351	1.976	1.986	1.919	1.927	1.840	1.845	1.721	1.723	1.649
5.00	2.601	2.645	2.192	2.205	2.123	2.133	2.030	2.036	1.887	1.890	1.801
6.00	2.894	2.941	2.411	2.429	2.330	2.342	2.221	2.227	2.053	2.056	1.951
7.00	3.189	3.236	2.631	2.650	2.538	2.551	2.410	2.417	2.218	2.221	2.102
8.00	3.481	3.530	2.851	2.870	2.747	2.760	2.602	2.609	2.385	2.389	2.254
9.00	3.771	3.821	3.071	3.090	2.953	2.967	2.791	2.799	2.551	2.555	2.406
10.00	4.060	4.110	3.289	3.309	3.159	3.173	2.981	2.989	2.721	2.725	2.561

*LS—Local similarity solution.
†LNS—Local non-similarity solution.

It follows that the ratio of equation (54) to equation (55) gives

$$\left.\frac{Q_c}{Q_p}\right|_{\lambda=1} = \frac{[-\theta'(\xi_0, 0, \lambda)]_{\lambda=1}}{[-\theta'(0, \lambda)]_{\lambda=1}}, \tag{56a}$$

and

$$\left.\frac{Q_c}{Q_p}\right|_{\lambda\neq 1} = \frac{(1+3\lambda)}{(1-\lambda)} \xi_L^{-(1+3\lambda)/(1-\lambda)} \times \int_0^{\xi_L} \frac{[-\theta'(\xi, 0, \lambda)]}{[-\theta'(0, \lambda)]} \xi^{4\lambda/(1-\lambda)} d\xi. \tag{56b}$$

Numerical integration was carried out for the integral in equation (56b) with $\lambda = 0$, 1/4, 1/3, 1/2 and 3/4 for the range of ξ_L from 0 to 10. It is found that (1) the values of Q_c/Q_p given by equation (56b) are practically independent of λ (within 4%) for both the local similarity and the local non-similarity solution; (2) the difference in values given by the local similarity and the non-local similarity solution is within 2% as is shown in Fig. 3. Thus we may conclude from the numerical results that

$$\left.\frac{Q_c}{Q_p}\right|_{\text{any }\lambda} \cong \frac{[-\theta'(\xi_0, 0, \lambda)]_{\lambda=1}}{[-\theta'(0, \lambda)]_{\lambda=1}}. \tag{57}$$

It follows that

$$Q_c \cong CSk_m A^{3/2}\left(\frac{\rho_\infty g\beta K}{\mu\alpha}\right)^{\frac{1}{2}}\left(\frac{2}{1+3\lambda}\right) L^{(1+3\lambda)/2}, \tag{58}$$

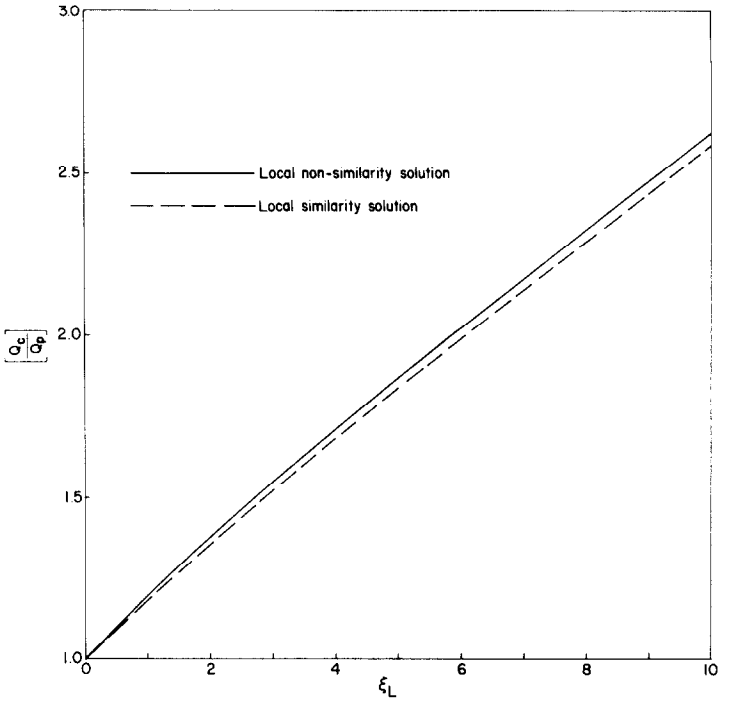

FIG. 3. Total heat-transfer ratio for any λ.

Table 3. Values of $C(\xi_L, \lambda)$ and $C(\xi_0)$

	$C(\xi_L, \lambda)$					$C(\xi_0)$
ξ_L or ξ_0	$\lambda = 0$	$\lambda = 1/4$	$\lambda = 1/3$	$\lambda = 1/2$	$\lambda = 3/4$	$\lambda = 1$
0.0	0.4440	0.6303	0.6788	0.7615	0.8926	1.000
0.5	0.4840	0.6900	0.7400	0.8300	0.9729	1.090
1.0	0.5230	0.7425	0.7996	0.8970	1.051	1.178
1.5	0.5603	0.7954	0.8566	0.9610	1.126	1.262
2.0	0.5962	0.8464	0.9116	1.023	1.199	1.343
2.5	0.6305	0.8950	0.9639	1.081	1.267	1.420
3.0	0.6642	0.9429	1.015	1.139	1.335	1.496
4.0	0.7322	1.039	1.119	1.256	1.472	1.649
5.0	0.7996	1.135	1.223	1.371	1.608	1.801
6.0	0.8662	1.230	1.324	1.486	1.741	1.951
7.0	0.9333	1.325	1.427	1.601	1.876	2.102
8.0	1.001	1.421	1.530	1.716	2.012	2.254
9.0	1.068	1.517	1.633	1.832	2.148	2.406
10.0	1.137	1.614	1.738	1.950	2.286	2.561

where the values of C, which is tabulated in Table 3, depends on ξ_L and λ for $\lambda \neq 1$, and depends on ξ_0 for $\lambda = 1$.

Acknowledgement—This study is part of the Hawaii Geothermal Project funded in part by the RANN program of the National Science Foundation of the United States (Grant No. GI-38319), the Energy Research and Development Administration of the United States (Grant No. E(04-3)-1093), and by the State and County of Hawaii.

REFERENCES

1. G. A. Macdonald, *Volcanoes*. Prentice-Hall, Englewood Cliffs, NJ (1972).
2. D. C. White, Characteristics of geothermal resources, in *Geothermal Energy Resources, Production, Stimulation*, edited by P. Kruger and C. Otte. Stanford University Press, Stanford (1973).
3. R. A. Wooding, Convection in a saturated porous medium at large Rayleigh number or Peclet number, *J. Fluid Mech.* **15**, 527–544 (1963).
4. A. McNabb, On convection in a porous medium, Proceedings of the 2nd Australasian Conference on Hydraulics and Fluid Mechanics, University of Auckland, New Zealand, C161–C171 (1965).
5. P. Cheng and W. J. Minkowycz, Similarity solution for free convection about a dike, Hawaii Geothermal Project Technical Report No. 10 (28 October 1975).
6. P. Cheng and I-Dee Chang, Buoyancy induced flows in a porous medium adjacent to impermeable horizontal surfaces, Hawaii Geothermal Project Technical Report No. 12 (November 1975).
7. E. M. Sparrow and H. S. Yu, Local non-similarity thermal boundary layer solutions, *J. Heat Transfer* **93**, 328–334 (1971).
8. W. J. Minkowycz and E. M. Sparrow, Local non-similar solutions for natural convection on a vertical cylinder, *J. Heat Transfer* **96**, 178–183 (1974).

CONVECTION NATURELLE AUTOUR D'UN CYLINDRE VERTICAL NOYE DANS UN MILIEU POREUX

Résumé—On effectue une analyse de la convection naturelle autour d'un cylindre vertical noyé dans un milieu poreux saturé, la température à la surface du cylindre variant suivant une fonction puissance x de la distance au bord d'attaque. Dans le cas particulier où la température de surface varie linéairement avec x, c'est à dire $\lambda = 1$, une solution exacte est obtenue dans le cadre des approximations de la couche limite. Pour les autres valeurs de λ, des solutions approchées sont obtenues à partir de modèles avec et sans hypothèse de similitude locale. Il apparait que les solutions en similitude locale sont suffisamment précises pour toutes les applications pratiques. On donne des expressions analytiques pour les flux thermiques pariétaux locaux et globaux.

FREIE KONVEKTION AN EINEM SENKRECHTEN- IN EIN PORÖSES MEDIUM EINGEBETTETEN ZYLINDER

Zusammenfassung—Die freie Konvektion an einem senkrechten, in ein gesättigtes poröses Medium eingebetteten Zylinder wird analytisch behandelt. Die Oberflächentemperatur des Zylinders ändert sich mit x^{λ}, einer Potenzfunktion des Abstandes von der Anströmkante. Im Rahmen der Grenzschichtnäherung wird eine exakte Lösung für den Spezialfall erhalten, daß sich die Oberflächentemperatur linear mit x, d. h. $\lambda = 1$ ändert. Für andere Werte von λ werden Näherungslösungen aufgrund von örtlichen Ähnlichkeits- und örtlichen Nichtähnlichkeitsmodellen erhalten. Es zeigt sich, daß die örtlichen Ähnlichkeitslösungen hinreichend genau für praktische Zwecke sind. Analytische Beziehungen für den örtlichen Oberflächen-Wärmestrom und den Gesamtoberflächen-Wärmestrom werden angegeben.

СВОБОДНАЯ КОНВЕКЦИЯ ВОКРУГ ВЕРТИКАЛЬНОГО ЦИЛИНДРА, ПОМЕЩЕННОГО В ПОРИСТУЮ СРЕДУ

Аннотация — Анализируется свободно-конвективное течение вокруг вертикального цилиндра, помещенного в насыщенную пористую среду, где температура поверхности цилиндра изменяется как x^{λ}, т. е. степенная функция расстояния от передней кромки. В приближении пограничного слоя получено точное решение для случая, когда температура поверхности изменяется линейно с изменением x, т. е. когда $\lambda = 1$. Для других значений λ получены приближенные решения, основанные на моделях локальной автомодельности и локальной неавтомодельности. Найдено, что основанные на локальной автомодельности решения являются достаточно точными для всех практических случаев. Получены аналитические выражения для локального и суммарного тепловых потоков на поверхности.